Hindawi Publishing Corporation
Journal of Nanomaterials
Volume 2008, Article ID 849745, 7 pages
doi:10.1155/2008/849745

Research Article

Synthesis and Elastic Characterization of Zinc Oxide Nanowires

M. P. Manoharan, A. V. Desai, G. Neely, and M. A. Haque

Department of Mechanical and Nuclear Engineering, The Pennsylvania State University, University Park, PA 16802, USA

Correspondence should be addressed to M. A. Haque, mah37@engr.psu.edu

Received 20 August 2007; Accepted 24 January 2008

Recommended by Jun Lou

Zinc oxide nanowires, nanobelts, and nanoneedles were synthesized using the vapor-liquid-solid technique. Young's modulus of the nanowires was measured by performing cantilever bending experiments on individual nanowires in situ inside a scanning electron microscope. The nanowires tested had diameters in the range of 200–750 nm. The average Young's modulus, measured to be 40 GPa, is about 30% of that reported at the bulk scale. The experimental results are discussed in light of the pronounced electromechanical coupling due to the piezoelectric nature of the material.

1. INTRODUCTION

Zinc oxide (ZnO) exhibits several unique properties, such as being a semiconductor and a piezoelectric material [1], and consequently, is used in a wide variety of sensors and actuators. ZnO nanostructures are being explored for a wide range of applications in nanoscale devices, such as nanogenerators [2], gas sensors [3], field emission transistors [4], nanocantilevers [5], and in biomedical systems, such as ultrasensitive DNA sequence detectors [6]. Apart from the technological significance of ZnO nanostructures, their quasi one-dimensional structure with diameters in the range of tens of nanometers to hundreds of nanometers makes them interesting from a scientific point of view. In this size range, they are expected to possess interesting physical properties and pronounced coupling that are quite different from their bulk counterpart [7].

Although ZnO nanowires are touted as the next generation materials for use in nanoscale systems [8], very few experimental investigations on their mechanical properties are reported in literature. The lack of experimental studies is mainly due to the challenges of material characterization at the nanoscale, such as (i) specimen manipulation, alignment, and gripping to achieve the desired boundary conditions, and (ii) application and measurement of force and displacement with very high resolution [1]. Additionally, ability to perform in situ experiments is important for nanoscale materials characterization. In situ experiments, usually conducted in analytical chambers such as the scanning or transmission electron microscope (SEM or TEM), enable direct visualization of the events as they occur, thus providing qualitative information along with quantitative data. In situ experiments also ensure accuracy of the experimental procedures, which is challenging to supervise at the nanoscale.

In this paper, we study the effect of temperature and gas flow rate on the growth of different zinc oxide nanostructures synthesized using the vapor-liquid-solid (VLS) technique and present experimental results on Young's modulus of single ZnO nanowires. The modulus was measured by bending the nanowire in a cantilever configuration inside a SEM, enabled for in situ observations. In Section 2, we review the main techniques in literature for mechanical characterization at the nanoscale, and experimental results on Young's modulus of zinc oxide nanostructures.

2. REVIEW OF NANOMECHANICAL EXPERIMENTAL TECHNIQUES AND YOUNG'S MODULUS VALUES FOR ZINC OXIDE NANOSTRUCTURES

One of the direct techniques to measure Young's modulus of materials is uniaxial tensile testing. However, it is difficult to adapt this technique for nanoscale material characterization, due to the reasons mentioned in Section 1. Microelectromechanical systems (MEMS) are used as test beds for characterizing the mechanical properties of nanostructures to circumvent some of these problems at the cost of complexity in

Table 1: Young's modulus values of ZnO nanostructures reported in literature.

No.	Young's modulus (GPa)	Nanostructure type	Reference	Technique
(1)	52	Nanobelts	[9]	Mechanical resonance in TEM
(2)	50	Nanobelts	[10]	TEM resonance
(4)	29 ± 8	Nanowire	[11]	AFM bending (vertical nanowires)
(5)	140–210 (size effect reported)	Nanowire	[12]	SEM resonance
(6)	58	Nanowire	[13]	TEM resonance
(7)	90–100	Nanowire	[14]	Nanoindentation
(8)	38.2 by AFM 31.3 by nanoindentation	Nanobelt	[15]	Nanoindentation and 3-point AFM bending
(9)	106 ± 25	Nanowire	[16]	Detecting resonance under an optical microscope
(10)	97 ± 18	Nanowire	[17]	Tensile and cantilever bending experiments, measured modulus only at fracture
(11)	117, 229 (100 nm diameter) 232, 454 (30 nm diameter)	Nanowire	[18]	Buckling of nanowires using nanoindentation

device design and fabrication [19–21]. Desai and Haque [1] have used the uniaxial tensile testing technique to measure Young's modulus of ZnO nanowires. It is interesting to note that the authors reported fracture strains as high as 15% for the nanowires, which is unusual considering that bulk ZnO is a brittle material at the bulk scale [22]. Young's modulus of nanowires can also be extracted from the resonant frequency of a single nanowire, induced by an alternating electric field. As examples, researchers have used this dynamic characterization technique to measure the modulus of zinc oxide nanowires [13], carbon nanotubes [23], and gallium nitride nanowires [24].

The quasi-static counterpart of the dynamic experiments essentially involves bending the nanowire specimen with a very soft spring (e.g., cantilever beam). The experiment is generally performed using an Atomic Force Microscope (AFM). Here, the deformation is primarily strain gradient dominant at the rigid support. Song et al. [11] and Hoffmann et al. [17] have used this technique to measure Young's modulus of ZnO nanowires. It is important to note that the effect of varying levels of strain gradient in these experiments (caused by bending) may result in significant deviation in the mechanical properties, because of the piezo-electric nature of the material. AFM-based experiments are popular techniques for mechanical characterization, because the stiffness of the tip is very small, and hence, the force measurement resolution is very high (on the order of nano-Newtons). However, understanding the tip-nanowire interaction is crucial for accurate and reliable experimental studies. For instance, friction (due to slipping) and van der Waals forces between the nanowire and tip will introduce errors in the measurement of mechanical properties [25]. The influence of these surface forces on the mechanical properties will be more significant in the case of smaller diameter (less than 30–40 nm) or high aspect ratio nanowires (greater than 100), where the magnitude of forces is very small (on the order of pico-Newtons to few nano-Newtons). It is also important to note that specimen geometry, crystallographic orientation, synthesis process, and the nature of experimental technique–uniform strain versus strain gradient-dominant and static versus dynamic deformation, all significantly affect the experimental results. Consequently, a huge spread is observed in Young's modulus values reported in literature for zinc oxide nanowires, as summarized in Table 1.

In this paper, we present results on in situ cantilever bending experiments inside a Focused Ion Beam–Scanning Electron Microscope (FIB-SEM) on ZnO nanowires. These experiments provide information on the elasticity of ZnO nanowires determined using a quasi-static and strain gradient-dominated technique. In situ experiments enabled us to observe the nanowires-tip interaction during the experiment. In Section 3, we discuss the synthesis process of zinc oxide nanowires.

3. NANOWIRE SYNTHESIS PROCESS

We synthesized the zinc oxide nanowires by the vapor-liquid-solid (VLS) mechanism [26] using gold as a catalyst. The

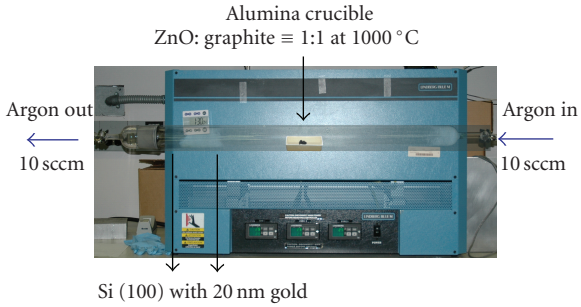

FIGURE 1: Vapor-liquid-solid synthesis chamber and process description.

Lindberg Anneal single tube furnace (Blue M) was used for the nanowire growth process; the schematic of the furnace is shown in Figure 1. We started with ZnO powder (Alfa Aesar, 99.99%) and graphite powder (Alfa Aesar, 99.99%) in 1 : 1 ratio by weight in an alumina crucible inside the furnace. Argon gas was allowed to flow in the tube (from right to left in Figure 1) at 10 sccm. The silicon (Si) substrates with 20 nm gold (Au) films (on [100] silicon surface) were placed downstream from the crucible, and served as the platform for nanowire growth.

As the temperature of the crucible increases to approximately 1000°C, the ZnO powder is reduced by graphite to form zinc (Zn), carbon monoxide (CO), and carbon dioxide (CO_2) vapors. The argon gas carries these vapor-phase products to the silicon samples placed at different temperatures. Meanwhile, gold and silicon droplets form a eutectic alloy at each catalyst site. The gaseous products produced by the reduction reaction adsorb and condense on the alloy droplets. Subsequently, the ZnO nanowire synthesis reaction is catalyzed by the Au-Si alloy at solid-liquid interface to form zinc oxide nanowires [27]. The ZnO vapor saturates the alloy droplet, followed by the nucleation and growth of solid ZnO nanowire, due to the super saturation of the liquid droplet. Incremental growth of the nanowire taking place at the droplet interface, constantly pushes the catalyst upwards until no more zinc vapor is available, or all the gold is used up. We observed nanowire growth from around 500°C to 900°C, the diameters of the nanowire ranged from 30 nm to 750 nm and the lengths were up to 100 μm. Some of the nanowires had a gold tip on the end (Figure 2(c)), indicating VLS mechanism for the growth process. We also observed nanobelt (Figure 2(a)) and nanoneedles (Figure 2(b)) formation in the lower-temperature regions. In Section 4, we discuss the sample preparation techniques for mechanical characterization experiments (cantilever bending) of nanowires.

4. SPECIMEN PREPARATION

The ZnO nanowires grown by VLS mechanism generally occurred as clusters, but individual nanowires are required for the experiments. Individual ZnO nanowires were picked using a micromanipulator (Creative Devices Inc., NJ, USA) fitted with an electrochemically sharpened tungsten probe tip. The nanowires adhere to the probe tip due to both short- and

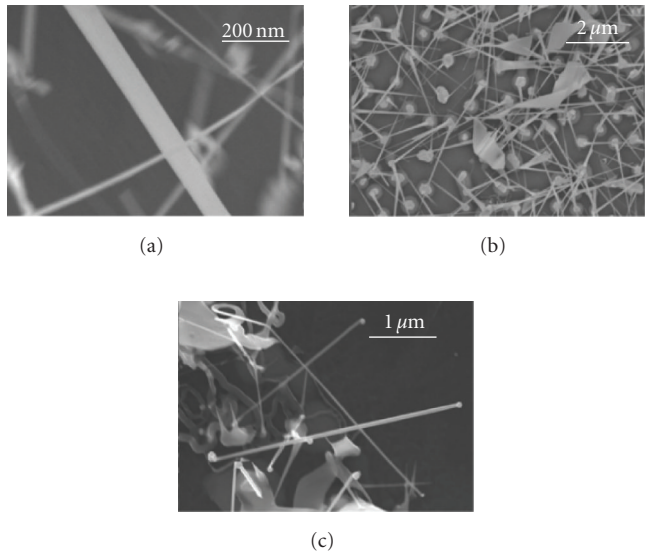

FIGURE 2: Effect of synthesis temperature on the geometry of nanostructures: (a) nanobelts at 650–700°C, (b) nanoneedles at 825–875°C, (c) nanowires at 900–950°C.

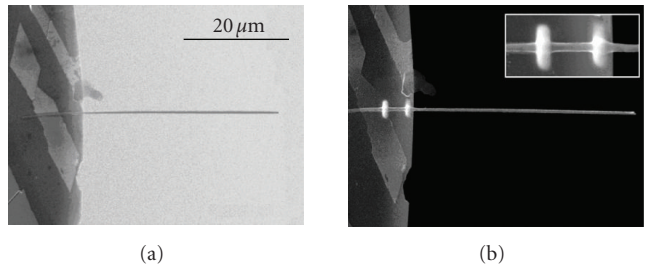

FIGURE 3: Zinc oxide nanowire (a) before and (b) after "gluing" with platinum in FIB-SEM. Inset in (b) shows platinum deposition on the nanowire near the edge of the wafer.

long-range attractive forces, which we generically term as van der Waal's forces. The nanowire was then placed on the edge of a chip of silicon wafer (coated with 100 nm thick gold film to improve imaging in SEM), as shown in Figure 3(a). The nanowire was oriented perpendicular to the edge of the silicon wafer using the probe tip. We "glued" the end of the nanowire near the edge of the silicon wafer by platinum deposition using a focused ion beam (FIB) (FEI Quanta 3D 200 FIB/SEM), as shown in Figure 3(b). The inset in Figure 3(b) shows the platinum deposition or "glue" on the nanowire near the edge of the silicon wafer. The microscale version of the pick-and-place technique is time intensive, but enables us to consistently prepare long nanowire specimens for the experiments. In Section 5, we discuss the experimental technique and results on Young's modulus of ZnO nanowires.

5. EXPERIMENTAL SETUP AND RESULTS

We performed cantilever-bending experiments to estimate Young's modulus of the nanowires. Bending loads were applied on the nanowires using an AFM cantilever with a

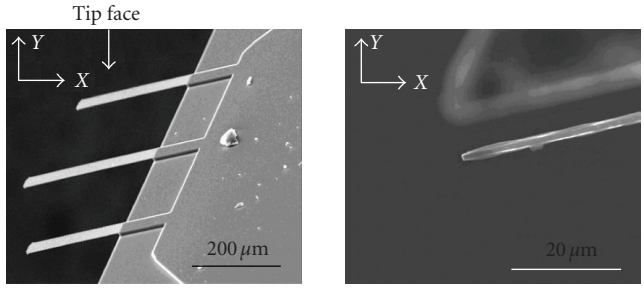

(a) (b)

Figure 4: (a) Tipless AFM cantilever (b) when mounted on the tungsten tip in the omniprobe.

known spring constant. The AFM cantilever (MikroMasch, CSC12) was mounted on the tungsten probe tip in the omniprobe (a three-axis piezoelectric actuator in the FIB-SEM) along the x-axis (Figure 4(a), probe is not shown in image). The SEM image plane is the X-Y plane.

We then tilted the probe such that the tip face was aligned perpendicular to the viewing screen (parallel to the Z-axis) (Figure 4(b)). This ensures that the loading direction is in the desired plane (X-Y plane).

We then mounted the nanowire specimen inside the SEM chamber, and rotated the SEM stage (about the Z-axis) to align the longitudinal axis (length) of the nanowire parallel to the length of the AFM cantilever (Figure 5(a)). This ensures that the central axis of the nanowire and AFM tip are parallel before loading. We then tilted the stage (around the x-axis) to verify that the nanowire is completely in the X-Y plane. After ensuring that the nanowire and the AFM tip were aligned, we performed the cantilever-bending experiment inside the SEM. The schematic of the bending experiment is shown in Figure 5(a). Note that Figure 5(a) is not to scale and in reality, the nanowire is thinner than the AFM cantilever. Figure 5(b) shows the in situ bending experiment inside the SEM.

The AFM cantilever moves vertically downwards (negative Y direction) to vertically load the nanowire and the deflection of the AFM cantilever and nanowire tip are the same. We can estimate Young's modulus of the nanowire from the deflections of the AFM cantilever base and nanowire tip.

We assume the following conditions for the cantilever bending experiments:

(1) clamped fixed end,
(2) small nanowire tip deflections (valid for $y_{nw}/l \leq 0.1$, where y_{nw} and l are the tip deflection and length of the nanowire, resp.).

Based on these assumptions, the normal or tensile bending stress (σ) and the normal or tensile bending strain (ε) on the nanowire, during the cantilever bending are given by

$$\sigma = \frac{32k_{tip}(y_{base} - y_{nw})l}{\pi d^3}, \qquad \varepsilon = \frac{3y_{nw}d}{2l^2}, \tag{1}$$

where k_{tip} is the stiffness of the AFM cantilever tip, y_{base} is the displacement of the AFM cantilever base, y_{nw} is the displacement of the nanowire, d is the diameter of the nanowire, and the stresses and strains are the maximum values that occur on the outermost diameter of the nanowire at the clamped end. The deflections of the nanowire and AFM cantilever base are estimated from processing the SEM images during the loading experiments. Thus, using the deflection values of the AFM cantilever base and nanowire tip and (1), we can estimate the normal stress and strain on the nanowire, and plot a stress-strain diagram. The slope of the stress-strain curve (linear fit) is Young's modulus of the nanowire. We performed cantilever bending experiments inside the SEM on ZnO nanowires specimens with diameters ranging from 350–750 nm and did not observe any dependence of Young's modulus on the diameter of the nanowire. Figure 6 shows a representative stress-strain diagram. Young's modulus values of the nanowires (five specimens) ranged from 35 GPa to 44 GPa, which is within the expected error in the experimental data. In some of the bending experiments, the deflections of the nanowires were large and the expressions for stress and strain (1) are not accurate. In those cases, the nonlinear moment curvature differential equation is numerically solved to match the bending profile of the nanowire to obtain more accurate values of the stresses and strains (details in [25]).

For mechanical measurements, the boundary condition of the cantilever support is critical for an accurate estimation of the properties. Typically, the nanowire specimen is clamped with electron-beam-induced deposition [28, 29] or the focused ion beam-based platinum deposition (FIB-Pt) [19], which might introduce ion beam induced stresses [25]. However, our in situ SEM observations show that for nanoscale bending experiments on specimens without deposition-based clamping, there is no observable rotation of the nanowire at the fixed end. This suggests that specimen-substrate adhesion could be strong enough to work as a clamping mechanism.

In order to study the effect of boundary conditions, we repeated the experiment on adhesion-clamped specimens prepared using the technique employed by Ding et al. [29]. From the experiments on adhesion-clamped specimens, we measured Young's modulus of the nanowires to vary from 18 GPa to 27 GPa (four specimens), and the range of diameters was from 200 nm to 330 nm. This discrepancy can be attributed largely to the difference in boundary conditions in the two specimen clamping techniques. If the applied bending force is comparable to the adhesion and friction forces, the rigid support boundary condition is no longer valid, as the nanowire has free boundary conditions on a significant part of its outer surface. In Section 6, the synthesis process and the experimental results are discussed.

6. DISCUSSION

We studied the effects of temperature on the synthesis of ZnO nanostructures using the VLS technique, and subsequently characterized their elastic properties. We observed no nanowire growth at gas flow rates higher than 10 sccm implying that the zinc, carbon monoxide, and carbon dioxide

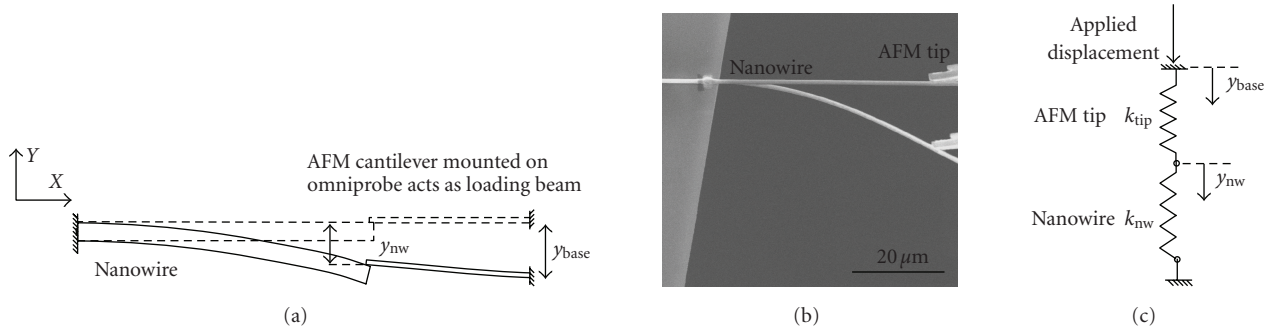

Figure 5: (a) Schematic of nanowire-bending experiment, (b) superimposed images from the in situ bending experiment inside the SEM showing the specimen and only the tip of the loading structure and (c) "spring" equivalent of the experimental setup.

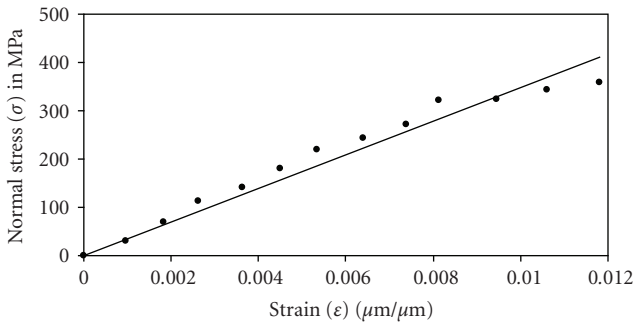

Figure 6: Stress-strain diagram for a ZnO nanowire specimen.

vapors are carried away rapidly from the substrates and do not have enough time to react at the silicon-gold interface. In most of the cases, the nanowire growth temperatures were between 500 and 800°C, which is consistent with the binary phase diagram of gold and zinc [30]. Ideally, the nanowire growth temperatures should be set between the eutectic temperature (683°C) for gold and zinc and melting point of zinc (420°C), reaching a maximum of 750°C [31]. However, it should be noted that the equilibrium phase diagrams at the nanoscale might be different from bulk and could result in different preferential growth temperatures for the nanowires. In some cases, we observed the growth of different nanostructures of zinc oxide such as nanobelts and nanoneedles (Figures 2(a) and 2(b)), similar to observations by other researchers [32, 33].

From transmission electron microscope (TEM) images, the growth direction of the nanowire was determined to be [0001], and the nanowires had a wurtzite crystal structure (single crystal) with lattice constants close to those of bulk crystals. At the bulk scale, Young's modulus of zinc oxide in the [0001] direction is 140 GPa [34], which is significantly higher than the modulus value reported in this paper. This is commonly attributed to the surface stress effects in the literature. Due to the lower coordination number of surface atoms compared to bulk atoms, there exist intrinsic surface stresses in materials [35, 36], and the mechanical properties of surfaces are different from bulk. The effects of surface stresses are significant when the size of the material is on the order of $h_0 = S/E$, where S is the surface elastic constant and E is the modulus of the bulk material [37]. For zinc oxide, the order of h_0 is approximately a few angstroms, which implies that the surface effects cannot alone explain the size effects observed in Table 1.

One of the reasons for the observed scatter in the modulus values (Table 1) is the difference in experimental techniques used to estimate Young's modulus. The dynamic experiments performed by Huang et al. [13], Chen et al. [12], and Zhou et al. [16] are expected to show slightly higher, unrelaxed (E_U) modulus, whereas in this paper we report modulus values estimated by quasi-static experiments (E_R). In dynamic experiments, the time period of motion of the nanowire is much lower than the relaxation time, and hence, the modulus values estimated during dynamic experiments tend to be higher than the values estimated during static or quasi-static experiments ($E_U > E_R$) [38]. Also, the oscillating electric field applied to the specimen induces charges on the nanowire surface, which can significantly overestimate the elastic properties [39]. For aspect ratios of around 100 for copper nanowires, the measured modulus could be 1.5 times the actual modulus.

The modulus value reported in this paper is less than the modulus value estimated by Feng et al. [14] (90–100 GPa), using nanoindentation. They estimated the modulus of the nanowires from the hardness values of the nanowires, which were measured during nanoindentation. In order to estimate the hardness of the nanowire, they had to make assumptions about the elastic properties of the nanoindenter tip and the nanowire material. In their experiments, they assumed that the elastic properties of bulk ZnO are applicable to ZnO nanowires, and this may have influenced the final estimated modulus value of the ZnO nanowire. Ni and Li [15] estimated the bending Young's modulus of ZnO nanobelts as 38.2 GPa and nanoindentation modulus as 31.1 GPa, which compare favorably with the modulus values reported in this paper.

A possible mechanism to explain the reduction in modulus of ZnO nanowire compared to bulk is the strong electromechanical coupling in zinc oxide. Due to its noncentrosymmetric wurtzite structure and ionic nature of the interatomic bond, internal electric fields are induced in ZnO when the material is strained [40, 41]. The positive sign

of the electromechanical coupling coefficient, e_{33}, along the [0001] direction implies that the induced electric field tends to reduce the measured modulus of the nanowire. Additional electrical polarization is introduced in the nanowire during flexural deformation due to the flexoelectric effect which arises because of the high-strain gradient at the nanoscale [42]. For piezoelectric materials with low dielectric constant, such as zinc oxide, quasi-static tests are not recommended for measurements of elastic constants (Young's modulus) because of the uncertainties in electrical boundary conditions [43]. As a result, the measured modulus values in quasi-static nanomechanical characterization (e.g., the technique reported in this paper) are influenced by the electromechanical coupling resulting in Young's modulus of ZnO nanowire being different from bulk. Another approach for explanation of reduction in modulus is that the elastic properties of a material can be described at the atomistic level, where the bond length, bond energy, and arrangement of atoms influence the overall elastic behavior of the material [44, 45]. In case of ZnO, the effective charge (e^*) on the zinc-oxygen changes due to charge redistribution when the material is strained [46]. Since Young's modulus of the material depends on e^*, the modulus of the material should change at higher strains. The techniques used for measuring the elastic properties at bulk scale involve negligible strains compared to nanoscale bending experiments. As a result, the measured modulus values of nanoscale zinc oxide are different from bulk due to strain-dependent modulus.

7. CONCLUSION

Zinc oxide nanostructures (nanobelts, nanoneedles, and nanowires) were synthesized using the vapor-liquid-solid technique. Young's modulus of the nanowires was estimated by bending experiments performed in situ in a scanning electron microscope on individual nanowires. Young's modulus was measured to be about 40 GPa, which is about 30% of the modulus value at the bulk scale (140 GPa). It was observed that the specimen preparation technique influences the boundary conditions, which affects the measured modulus value. The observed size effect was discussed on the basis of the pronounced electromechanical coupling and strain gradient at the nanoscale.

ACKNOWLEDGMENTS

The authors acknowledge support from the National Science Foundation (CMMI-0555420 and ECCS-0501436). This publication was supported by the Pennsylvania State University Materials Research Institute Nano Fabrication Network and the National Science Foundation Cooperative Agreement no. 0335765, National Nanotechnology Infrastructure Network, with Cornell University.

REFERENCES

[1] A. V. Desai and M. A. Haque, "Mechanical properties of ZnO nanowires," *Sensors and Actuators A*, vol. 134, no. 1, pp. 169–176, 2007.

[2] X. Wang, J. Song, and Z. L. Wang, "Nanowire and nanobelt arrays of zinc oxide from synthesis to properties and to novel devices," *Journal of Materials Chemistry*, vol. 17, no. 8, pp. 711–720, 2007.

[3] E. Comini, G. Faglia, G. Sberveglieri, Z. Pan, and Z. L. Wang, "Stable and highly sensitive gas sensors based on semiconducting oxide nanobelts," *Applied Physics Letters*, vol. 81, no. 10, pp. 1869–1871, 2002.

[4] M. S. Arnold, P. Avouris, Z. W. Pan, and Z. L. Wang, "Field-effect transistors based on single semiconducting oxide nanobelts," *Journal of Physical Chemistry B*, vol. 107, no. 3, pp. 659–663, 2003.

[5] W. L. Hughes and Z. L. Wang, "Nanobelts as nanocantilevers," *Applied Physics Letters*, vol. 82, no. 17, pp. 2886–2888, 2003.

[6] N. Kumar, A. Dorfman, and J.-I. Hahm, "Ultrasensitive DNA sequence detection using nanoscale ZnO sensor arrays," *Nanotechnology*, vol. 17, no. 12, pp. 2875–2881, 2006.

[7] M. Law, J. Goldberger, and P. Yang, "Semiconductor nanowires and nanotubes," *Annual Review of Materials Research*, vol. 34, no. 1, pp. 83–122, 2004.

[8] Y. Xia, P. Yang, Y. Sun, et al., "One-dimensional nanostructures: synthesis, characterization, and applications," *Advanced Materials*, vol. 15, no. 5, pp. 353–389, 2003.

[9] Z. L. Wang, "Zinc oxide nanostructures: growth, properties and applications," *Journal of Physics: Condensed Matter*, vol. 16, no. 25, pp. R829–R858, 2004.

[10] X. D. Bai, P. X. Gao, Z. L. Wang, and E. G. Wang, "Dual-mode mechanical resonance of individual ZnO nanobelts," *Applied Physics Letters*, vol. 82, no. 26, pp. 4806–4808, 2003.

[11] J. Song, X. Wang, E. Riedo, and Z. L. Wang, "Elastic property of vertically aligned nanowires," *Nano Letters*, vol. 5, no. 10, pp. 1954–1958, 2005.

[12] C. Q. Chen, Y. Shi, Y. S. Zhang, J. Zhu, and Y. J. Yan, "Size dependence of Young's modulus in ZnO nanowires," *Physical Review Letters*, vol. 96, no. 7, Article ID 075505, 4 pages, 2006.

[13] Y. Huang, X. Bai, and Y. Zhang, "*In situ* mechanical properties of individual ZnO nanowires and the mass measurement of nanoparticles," *Journal of Physics: Condensed Matter*, vol. 18, no. 15, pp. L179–L184, 2006.

[14] G. Feng, W. D. Nix, Y. Yoon, and C. J. Lee, "A study of the mechanical properties of nanowires using nanoindentation," *Journal of Applied Physics*, vol. 99, no. 7, Article ID 074304, 10 pages, 2006.

[15] H. Ni and X. Li, "Young's modulus of ZnO nanobelts measured using atomic force microscopy and nanoindentation techniques," *Nanotechnology*, vol. 17, no. 14, pp. 3591–3597, 2006.

[16] J. Zhou, C. S. Lao, P. Gao, et al., "Nanowire as pico-gram balance at workplace atmosphere," *Solid State Communications*, vol. 139, no. 5, pp. 222–226, 2006.

[17] S. Hoffmann, F. Östlund, J. Michler, et al., "Fracture strength and Young's modulus of ZnO nanowires," *Nanotechnology*, vol. 18, no. 20, Article ID 205503, 5 pages, 2007.

[18] L.-W. Ji, S.-J. Young, T.-H. Fang, and C.-H. Liu, "Buckling characterization of vertical ZnO nanowires using nanoindentation," *Applied Physics Letters*, vol. 90, no. 3, Article ID 033109, 3 pages, 2007.

[19] Y. Zhu and H. D. Espinosa, "An electromechanical material testing system for *in situ* electron microscopy and applications," *Proceedings of the National Academy of Sciences of the United States of America*, vol. 102, no. 41, pp. 14503–14508, 2005.

[20] B. G. Demczyk, Y. M. Wang, J. Cumings, et al., "Direct mechanical measurement of the tensile strength and elastic modulus of multiwalled carbon nanotubes," *Materials Science and Engineering A*, vol. 334, no. 1-2, pp. 173–178, 2002.

[21] M. A. Haque and M. T. A. Saif, "*In situ* tensile testing of nanoscale freestanding thin films inside a transmission electron microscope," *Journal of Materials Research*, vol. 20, no. 7, pp. 1769–1777, 2005.

[22] S. Boggs, J. Kuang, H. Andoh, and S. Nishiwaki, "Electro-thermal-mechanical computations in ZnO arrester elements," *IEEE Transactions on Power Delivery*, vol. 15, no. 1, pp. 128–134, 2000.

[23] R. Ciocan, J. Gaillard, M. J. Skove, and A. M. Rao, "Determination of the bending modulus of an individual multiwall carbon nanotube using an electric harmonic detection of resonance technique," *Nano Letters*, vol. 5, no. 12, pp. 2389–2393, 2005.

[24] C.-Y. Nam, P. Jaroenapibal, D. Tham, D. E. Luzzi, S. Evoy, and J. E. Fischer, "Diameter-dependent electromechanical properties of GaN nanowires," *Nano Letters*, vol. 6, no. 2, pp. 153–158, 2006.

[25] A. V. Desai and M. A. Haque, "Sliding of zinc oxide nanowires on silicon substrate," *Applied Physics Letters*, vol. 90, no. 3, Article ID 033102, 3 pages, 2007.

[26] P. Yang, H. Yan, S. Mao, et al., "Controlled growth of ZnO nanowires and their optical properties," *Advanced Functional Materials*, vol. 12, no. 5, pp. 323–331, 2002.

[27] C. Y. Lee, T. Y. Tseng, S. Y. Li, and P. Lin, "Growth of zinc oxide nanowires on silicon (100)," *Tamkang Journal of Science and Engineering*, vol. 6, no. 2, pp. 127–132, 2003.

[28] D. A. Dikin, X. Chen, W. Ding, G. Wagner, and R. S. Ruoff, "Resonance vibration of amorphous SiO_2 nanowires driven by mechanical or electrical field excitation," *Journal of Applied Physics*, vol. 93, no. 1, pp. 226–230, 2003.

[29] W. Ding, L. Calabri, X. Chen, K. M. Kohlhaas, and R. S. Ruoff, "Mechanics of crystalline boron nanowires," *Composites Science and Technology*, vol. 66, no. 9, pp. 1112–1124, 2006.

[30] H. Okamoto and T. B. Massalski, *Phase Diagrams of Binary Gold Alloys*, ASM International, Materials Park, Ohio, USA, 1987.

[31] Y. Wu, H. Yan, M. Huang, B. Messer, J. H. Song, and P. Yang, "Inorganic semiconductor nanowires: rational growth, assembly, and novel properties," *Chemistry: A European Journal*, vol. 8, no. 6, pp. 1261–1268, 2002.

[32] Z. L. Wang, "Nanostructures of zinc oxide," *Materials Today*, vol. 7, no. 6, pp. 26–33, 2004.

[33] J. Y. Lao, J. Y. Huang, D. Z. Wang, and Z. F. Ren, "ZnO nanobridges and nanonails," *Nano Letters*, vol. 3, no. 2, pp. 235–238, 2003.

[34] I. B. Kobiakov, "Elastic, piezoelectric and dielectric properties of ZnO and CdS single crystals in a wide range of temperatures," *Solid State Communications*, vol. 35, no. 3, pp. 305–310, 1980.

[35] R. Dingreville, J. Qu, and M. Cherkaoui, "Surface free energy and its effect on the elastic behavior of nano-sized particles, wires and films," *Journal of the Mechanics and Physics of Solids*, vol. 53, no. 8, pp. 1827–1854, 2005.

[36] W. Haiss, "Surface stress of clean and adsorbate-covered solids," *Reports on Progress in Physics*, vol. 64, no. 5, pp. 591–648, 2001.

[37] V. B. Shenoy, "Atomistic calculations of elastic properties of metallic fcc crystal surfaces," *Physical Review B*, vol. 71, no. 9, Article ID 094104, 11 pages, 2005.

[38] A. S. Nowick and B. S. Berry, *Analelastic Relaxation in Crystalline Solids*, Academic Press, New York, NY, USA, 1972.

[39] X. Zheng and L. Zhu, "Theoretical analysis of electric field effect on Young's modulus of nanowires," *Applied Physics Letters*, vol. 89, no. 15, Article ID 153110, 3 pages, 2006.

[40] A. Sakamoto and T. Ogawa, "Effective charge in the IIVI and IIIV compounds with zincblende or wurtzite type structure," *Journal of Physics and Chemistry of Solids*, vol. 36, no. 6, pp. 583–589, 1975.

[41] R. Kato and J. Hama, "First-principles calculation of the elastic stiffness tensor of aluminium nitride under high pressure," *Journal of Physics: Condensed Matter*, vol. 6, no. 38, pp. 7617–7632, 1994.

[42] R. Maranganti, N. D. Sharma, and P. Sharma, "Electromechanical coupling in nonpiezoelectric materials due to nanoscale nonlocal size effects: Green's function solutions and embedded inclusions," *Physical Review B*, vol. 74, no. 1, Article ID 014110, 14 pages, 2006.

[43] ANSI/IEEE Std 176-1987, "IEEE standard on piezoelectricity," The Institute of Electrical and Electronics Engineers: New York, NY, USA, 1987.

[44] R. M. Martin, "Elastic properties of ZnS structure semiconductors," *Physical Review B*, vol. 1, no. 10, pp. 4005–4011, 1970.

[45] R. M. Martin, "Relation between elastic tensors of wurtzite and zincblende structure materials," *Physical Review B*, vol. 6, no. 12, pp. 4546–4553, 1972.

[46] J. C. Phillips and J. A. Van Vechten, "Charge redistribution and piezoelectric constants," *Physical Review Letters*, vol. 23, no. 19, pp. 1115–1117, 1969.